THE JOURNAL OF PHYSICAL CHEMISTRY Letters

pubs.acs.org/JPCL Letter

"Watching" a Molecular Twist in a Protein by Raman Optical Activity

Junpei Matsuo, Takashi Kikukawa, Tomotsumi Fujisawa, Wouter D. Hoff, and Masashi Unno*

Cite This: *J. Phys. Chem. Lett.* 2020, 11, 8579–8584 Read Online

ACCESS | Metrics & More | Article Recommendations | Supporting Information

ABSTRACT: Light-absorbing chromophores in photoreceptors contain a π-electron system and are intrinsically planar molecules. However, within a protein environment these cofactors often become nonplanar and chiral in a manner that is widely believed to be functionally important. When the same chromophore is out-of-plane distorted in opposite directions in different members of a protein family, such conformers become a set of enantiomers. In techniques using chiral optical spectroscopy such as Raman optical activity (ROA), such proteins are expected to show opposite signs in their spectra. Here we use two microbial rhodopsins, *Gloeobacter* rhodopsin and sodium ion pump rhodopsin (NaR), to provide the first experimental and theoretical evidence that the twist direction of the retinal chromophore indeed determines the sign of the ROA spectrum. We disrupt the hydrogen bond responsible for the distortion of the retinal in NaR and show that the sign of the ROA signals of this nonfunctional mutant is flipped. The reported ROA spectra are monosignate, a property that has been seen for a variety of photoreceptors, which we attribute to an energetically favorable gradual curvature of the chromophore.

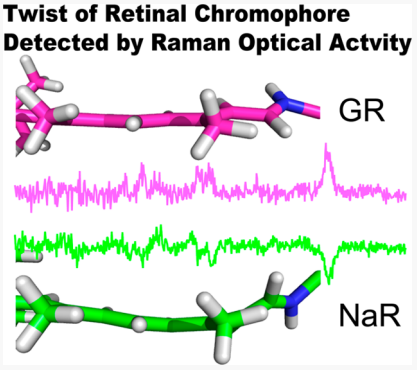

Many proteins contain functionally important cofactors. Light-absorbing chromophores at the active site of a photoreceptor protein provide classic examples that have been used extensively to understand protein−cofactor interactions. A protein matrix often causes a structural distortion of the chromophore, and such altered structures are widely considered to be important for biological function. For instance, the out-of-plane distortion of a protein-embedded chromophore has been identified as a crucial factor in tuning their absorption spectra.[1,2] Furthermore, in visual rhodopsin and related proteins, the primary intermediate formed upon light absorption contains a chromophore that is highly out-of-plane distorted.[3,4] This structural distortion can store light energy to drive subsequent protein conformational changes.[5] However, experimentally detecting the small atomic displacements that cause such distortions is challenging.

Raman optical activity (ROA) is an emerging spectroscopic technique that provides chiral sensitivity.[6−10] It measures the difference in Raman scattering intensity between right (I^R) and left (I^L) circularly polarized incident light, where the sum of I^R and I^L is the parent Raman spectrum. This original form is called incident circular polarization (ICP) ROA. The ROA spectrum can also be measured by detecting the right (I_R) and left (I_L) components in Raman scattered lights,[11] which is called scattered circular polarization (SCP) ROA. The method can be applied to chromophoric proteins, and recent progress has shown that this technique is a promising approach for detecting the distortion of a chromophore within a protein environment.[12−16] When a chromophore is out-of-plane distorted in opposite directions, the two different structures are enantiomers of each other. We therefore expected that their ROA spectra would exhibit opposite signs. In fact, quantum chemical calculations based on density functional theory (DFT) demonstrated that the sign of an ROA band reports the direction of the distortion, while its amplitude is proportional to the degree of the distortion.[16] Whereas this computational result is reasonable, its experimental verification has not been reported. One approach is to engineer a set of proteins containing a chromophore that is twisted in opposite directions. Here we focus on two functionally distinct microbial rhodopsins and experimentally demonstrate that the distortion of their chromophore in opposite directions indeed yields ROA signals with opposite sign. Furthermore, we present an example showing that this technique is capable of detecting a functionally important conformational change in the enantiomorphic state of a chromophore caused by an amino acid replacement.

In this study, we utilize light-driven proton pump *Gloeobacter* rhodopsin (GR) from cyanobacterium *Gloeobacter violaceus*[17] and a sodium-ion-pumping rhodopsin[18] from *Indibacter alkaliphilus* (*Ia*NaR). GR contains all-trans retinal as a chromophore (Figure 1A), and the crystal structure demonstrates that its protonated Schiff base NH moiety forms a hydrogen bond with a water molecule (Figure 1B).[19] NaR also contains all-trans retinal, but the crystal structure of

Received: August 10, 2020
Accepted: September 18, 2020
Published: September 18, 2020

https://dx.doi.org/10.1021/acs.jpclett.0c02448
J. Phys. Chem. Lett. 2020, 11, 8579−8584

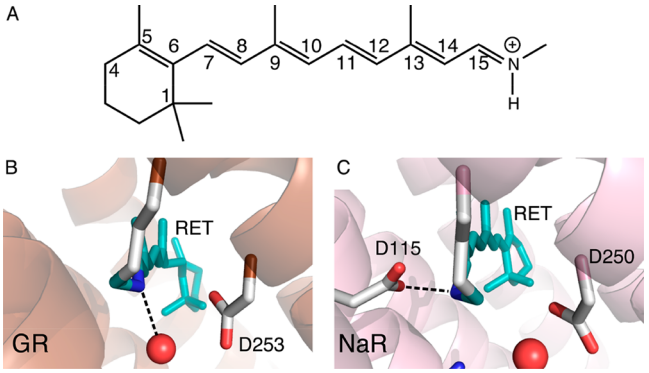

Figure 1. Structures of the all-trans retinal chromophore and the active site of GR and NaR. (A) All-trans retinal protonated Schiff base. (B, C) Active-site structures of GR and NaR (KR2) based on their crystal structures.[19,20] RET indicates the retinal chromophore. In panel C, a corresponding residue for NaR from *Indibacter alkaliphilus* is indicated. PDB codes: 6NWD (GR) and 3X3C (KR2). Hydrogen bonding interactions at the Schiff base NH moiety are illustrated by dotted lines.

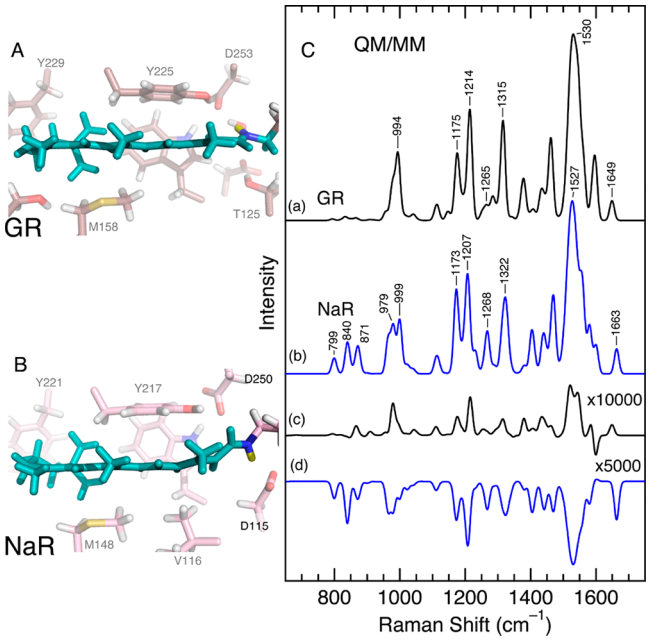

Figure 2. Optimized structures and simulated Raman and ROA spectra for GR and NaR. Optimized geometries of the active site for (A) GR and (B) NaR. The retinal cofactor is illustrated in teal, and its protonated Schiff base moiety is colored blue (nitrogen) and yellow (hydrogen). In panel B, the residue number for *Ia*NaR is used. (C) Raman (a, b) and ROA (c, d) spectra determined for models GR and NaR using QM/MM calculations are shown. Gaussian band shapes with a 10 cm^{-1} width were used except for a 20 cm^{-1} width for the highest bands at around 1530 cm^{-1} (1529 cm^{-1} for GR; 1522 and 1540 cm^{-1} for NaR). Raman and ROA intensities for these bands were reduced by a factor of 4 to make the other bands visible.

Krokinobacter eikastus rhodopsin 2 (KR2) revealed that the Schiff base NH moiety forms a hydrogen bond with an aspartate located on the opposite side of the retinal (Asp115 for *Ia*NaR) (Figure 1C).[20,21] This is an ionic hydrogen bond, which is stronger than a standard hydrogen bond.[22] Because of this strong interaction, the retinal NH group points toward the aspartate, leading to an oppositely out-of-plane distorted chromophore in NaR compared to that of GR. We therefore expect that the ROA spectra are also opposite in sign between the two proteins.

To explore the idea that the signs of the ROA bands are opposite between GR and NaR, we first performed quantum chemical calculations to predict the signs of their ROA bands. The initial starting geometries were taken from the crystal structures of GR[19] and KR2,[20] and water molecules near the surface of the protein were removed. The entire system was partially optimized at the B3LYP/6-31+G**:Amber level of a quantum mechanics/molecular mechanics (QM/MM) calculation. (For details, see the Supporting Information.) In the partial optimization, only the QM part (retinal chromophore) was optimized, and these structures are denoted as models GR and NaR. The active-site structures for these models are compared in Figure 2A,B, illustrating that the Schiff base NH moiety orients in opposite directions in the two models. We used these models to simulate the Raman and ROA spectra using an excitation wavelength of 785 nm (Figure 2C). The band assignments are summarized in the Supporting Information. The computed Raman spectra (traces a and b) are quite similar to each other. In contrast, the calculated ROA bands for GR and NaR are opposite in sign, i.e., most of the ROA bands for model GR are positive, while model NaR exhibits negative ROA bands.

To experimentally test these theoretical predictions, we measured the Raman ($I_R + I_L$) and ROA ($I_R - I_L$) spectra of GR and NaR with 785 nm excitation under preresonance conditions for the retinal. In the present study, we used a newly developed SCP-ROA spectrometer, and its technical details are given in the Supporting Information. The upper two traces in Figure 3 are the observed Raman spectra of GR (trace a) and *Ia*NaR (trace b). Their overall spectral features are similar. Both proteins show the ethylenic C=C stretch ($\nu_{C=C}$) at 1531−1532 cm^{-1} and the characteristic CH_3 rock (δ_{CH_3}), C−C (ν_{C-C}), and C=N ($\nu_{C=N}$) stretches at 1009, 1168/1201, and ∼1640 cm^{-1}, respectively.[23] These results are consistent with reported resonance Raman spectra for these proteins,[24,25] indicating a preresonance enhancement of the spectra of the retinal chromophore.[26]

The lower part of Figure 3 displays the ROA spectra of GR and NaR. In contrast to the parent Raman spectra, their ROA spectra are clearly different. The ROA spectrum of GR is characterized by positive bands for $\nu_{C=C}$, ν_{C-C}, and δ_{CH_3}, whereas the corresponding bands for NaR are all negative. In addition, both GR and NaR exhibit a positive and a negative ROA band near 960 cm^{-1}, respectively, although their corresponding Raman intensities are weak. This band is assigned to the hydrogen out-of-plane (HOOP) mode,[23,24] which acts as a spectroscopic ruler for measuring structural deformations of a chromophore molecule in a protein active site.[16] These observations provide experimental evidence for the proposal that the sign of the ROA spectra reflects the direction of the out-of-plane distortion of the retinal chromophore.

As discussed above, the unusual conformation of the retinal chromophore in NaR is due to a strong hydrogen bond between the positively charged Schiff base NH and a negatively charged carboxylate group of aspartate (Asp115). To further explore the role of this hydrogen bond, we attempted to weaken it by creating the D115N mutant, where a COO^- group is replaced with a neutral carbamoyl C=O(NH_2) group. This perturbation would be expected to reduce the

https://dx.doi.org/10.1021/acs.jpclett.0c02448
J. Phys. Chem. Lett. 2020, 11, 8579−8584

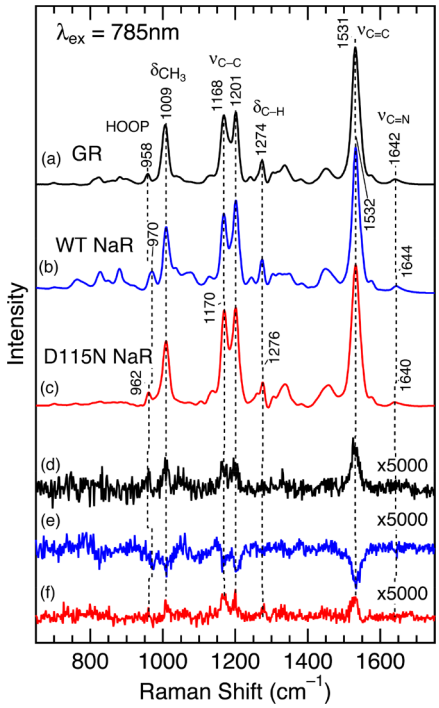

Figure 3. Raman and ROA spectra of GR and *Ia*NaR with 785 nm excitation. Spectra for (a, d) GR in a 10 mM three-mixture buffer, 400 mM NaCl, and 0.05% DDM at pH 8.5, (b, e) wild-type *Ia*NaR in 50 mM Tris-HCl, 400 mM NaCl, and 0.05% DDM at pH 8.0, and (c, f) the D115N mutant of *Ia*NaR in 50 mM Tris-HCl, 400 mM NaCl, and 0.05% DDM at pH 8.0. Traces a−c are Raman spectra. Traces d−e are ROA spectra, and their intensities are magnified by a factor of 5000.

degree of twist around the NH group, leading to a more planar retinal chromophore and thus reduced intensities in its ROA spectrum. In fact, recent X-ray crystallographic data for this mutant of KR2 were interpreted in terms of the coexistence of two alternative orientations of the retinal Schiff base: in one of them, the NH group is pointed toward Asp115, while the NH moiety flips and orients toward Asp250 in the second conformation.[27] To verify the effect of this mutation on the structure of the retinal chromophore, we measured the Raman and ROA spectra of the mutant. Traces b and c in Figure 3 demonstrate that the overall spectral features in the Raman spectra are similar between wild type (WT) and the D115N mutant, indicating that the mutant maintains the retinal configuration in an all-trans form. There are, however, two noticeable effects of the mutation on the spectrum. First, the intensities of the HOOP bands below 1000 cm^{-1} are reduced in the D115N mutant. Their lower intensities suggest that the deformation of the chromophore is reduced by the mutation. Second, a $\nu_{C=N}$ band at 1644 cm^{-1} is downshifted by 4 cm^{-1} upon the D115 mutation. This small downshift of $\nu_{C=N}$ can be interpreted in terms of a weakened hydrogen bond at the Schiff base NH moiety.[28]

In contrast to the Raman spectrum, the D115N mutation has a dramatic impact on the ROA spectrum and causes a flip in sign from negative to positive with reduced intensities (Figure 3, trace e → f). The reversed sign demonstrates that the weakening of the hydrogen bond at the Schiff base NH in the NaR mutant converts the retinal chromophore into a GR-like conformation. The reduced intensities can be correlated with the presence of two alternative conformations that show opposite signs in their ROA spectra since the positive and negative bands can be cancelled to yield net small positive bands. These observations are fully consistent both with the anticipated results of the mutation and with the crystallographic analysis of the mutant.[27] The net positive ROA bands imply that the GR-like retinal structure, where the Schiff base NH faces Asp250, is a main conformation in the mutant. Here we discuss the functional relevance of these findings for D115N. First, this mutation causes a red shift in the absorption maximum (Figure S3 in the Supporting Information),[18] indicating the significance of Asp115 for the color-tuning mechanism in NaR. Importantly, Inoue et al. reported that both sodium ion and proton-pumping activities are completely lost in this mutant.[18] The latter observation indicates that the hydrogen bonding interaction between Asp115 and the protonated Schiff base is crucial to the function of NaR. We conclude that the ROA spectroscopy successfully showed the detection of a conformational twist of the retinal chromophore that is related to the function of NaR.

Next, we discuss a general feature of the ROA spectra of photoreceptor proteins. Although "normal" ROA spectra are bisignate, having both positive and negative signs, the spectra for GR and NaR are monosignate (Figure 3). Similar monosignate spectra have been reported for a diverse group of other photoreceptor proteins, including photoactive yellow protein (PYP) containing a *p*-coumaric acid chromophore[13,16,26] and orange carotenoid protein (OCP) using a carotenoid as a cofactor.[15] A monosignate spectrum is a characteristic feature for the ROA spectra under resonance conditions in the single electronic state (SES) limit. A theoretical study by Nafie predicted that the resonance ROA (RROA) spectra in the SES limit are monosignate and have bands with the same relative intensities as those in the corresponding resonance Raman spectra.[29] In addition, the RROA spectrum is opposite in sign to the electronic circular dichroism (ECD) spectrum of the resonant electronic transition, and the ratio of the RROA to the resonance Raman spectrum is proportional to that of the ECD and parent absorption spectra. These predictions were experimentally proven.[26] In the cases of GR and NaR, although all ROA bands have the same sign, their relative intensities are not identical to those of the corresponding Raman bands. As displayed in Figure 3 and Figure S4 in the Supporting Information, the HOOP bands near 960 cm^{-1} in their ROA spectra are more intense compared to the other in-plane vibrational modes. The larger ROA intensities of the HOOP modes were also reported for PYP and OCP. On the basis of these observations, the monosignate spectra are not simple RROA spectra under the SES condition.

To examine the origin of the monosignate ROA spectra, we performed further DFT calculations. We used *N*-1,3-butadienyl-formiminium as a simple chromophore model (Figure 4, inset) and considered this molecule in three distinct conformations (Table S2 in the Supporting Information). A full geometry optimization resulted in a planar structure, which is denoted as model 1. The calculated Raman spectrum at the B3LYP/6-31+G** level is illustrated in Figure 4 (trace a, black). Since model 1 is achiral, the calculated ROA intensities were all zero. We also consider model 2, where the central C3═C4 bond is twisted by 30° (τ(N2−C3−C4−C5) = 150°), resulting in a molecule with a sharp kink in the middle. Its calculated Raman and ROA spectra are shown in Figure 4 (traces a and b, cyan). Model 2 is chiral, and its simulated

https://dx.doi.org/10.1021/acs.jpclett.0c02448
J. Phys. Chem. Lett. 2020, 11, 8579−8584

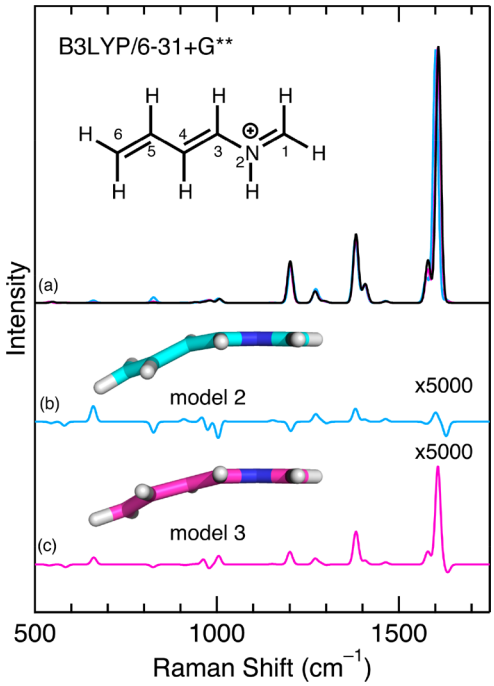

Figure 4. Simulated Raman and ROA spectra of models 1−3 in vacuo with 785 nm excitation. Gaussian band shapes with a 10 cm^{-1} width are used. (a) Raman spectra for models 1 (black), 2 (cyan), and 3 (magenta). (b, c) ROA spectra for models 2 and 3. The ROA spectra are magnified by a factor of 5000. Inset in (a): chemical structure of *N*-1,3-butadienyl-formiminium and (b, c) stick representations of models 2 and 3.

spectrum exhibits a typical spectral feature for ROA, having both positive and negative bands. In model 3, three dihedral angles, τ(C1−N2−C3−C4) = −165°, τ(N2−C3−C4−C5) = 165°, and τ(C3−C4−C5−C6) = −165°, were fixed, yielding a molecule with a gradual overall curvature (Figure 4, inset). In contrast to model 2, the ROA bands for model 3 are mostly positive, and the spectral feature showing the same sign in ROA spectra is analogous to that for GR and NaR.

The above results indicate that a bent molecule with a significant twist along a specific C=C bond (model 2) exhibits a "normal" bisignate ROA spectrum, while a monosignate spectrum is achieved for a curved molecule that exhibits an overall curvature caused by twists over multiple bonds (model 3). As illustrated in Figure S5 in the Supporting Information, the atomic positions in models 2 and 3 are quite similar. However, their energies are different: model 3 is more stable compared to model 2 by ∼13 kJ mol^{-1} (Table S2), which corresponds to approximately one classic hydrogen bond. Figure S6 in the Supporting Information displays the relative energies ΔE compared with the planar geometry of model 1. This analysis reveals that the distortion energy for the central C3=C4 double bond shows a parabolic dependency. This parabolic dependence accounts for the fact that the curved geometry having multiple twists is energetically more favorable. We propose that the monosignate ROA spectra observed for photoreceptor proteins are caused by the phenomenon that asymmetrically distorted cofactors which are gradually curved (as opposed to sharply kinked) are energetically preferred.

Finally, we further examine the origin of a monosignate ROA spectrum in a gradually curved molecule such as model 3. Figure S7 in the Supporting Information displays the simulated electronic absorption and ECD spectra of models 1−3. Although the out-of-plane distortions of the molecule exhibit a minor effect on the absorption spectrum, the calculated ECD spectra are significantly changed. Models 2 and 3 have negative ECD signals for the first ($S_0 \rightarrow S_1$ at 330 nm) and second ($S_0 \rightarrow S_2$ at ∼225 nm) lowest $\pi\pi^*$ transitions, while the third $S_0 \rightarrow S_3$ transition at ∼215 nm shows a positive sign. Notably, model 3 shows large negative signals for the lower-energy $S_0 \rightarrow S_1$ and $S_0 \rightarrow S_2$ transitions. We also examined the effect of the excitation wavelength on the Raman and ROA spectra of models 2 and 3, and the results are summarized in Figures S8 and S9 in the Supporting Information. In model 2, its ROA spectra have both positive and negative bands in the wide range of excitation wavelengths. The small negative ECD signals for $S_0 \rightarrow S_1$ and $S_0 \rightarrow S_2$ lead to a relatively large contribution of $S_0 \rightarrow S_3$ that has a positive ECD band. These situations account for the bisignate nature of the ROA spectra. On the other hand, the calculated ROA spectra for model 3 are mostly positive, which can be interpreted in terms of major contributions of the $S_0 \rightarrow S_1$ and $S_0 \rightarrow S_2$ transitions that have large negative ECD signals. These results indicate that a gradually curved molecule exhibits a large ECD signal for its $\pi\pi^*$ transition. In this case, the lowest-energy $\pi\pi^*$ transition mainly contributes to the ROA intensities; therefore, a monsignate spectrum that is characteristic of the RROA spectrum under the SES limit is achieved.

In summary, the present study demonstrated that ROA spectroscopy can "watch" the twist of a cofactor molecule in a protein with the sign of the ROA signal. The method provides a powerful approach to detecting functionally important conformational details in a protein active site.

■ ASSOCIATED CONTENT

Supporting Information

The Supporting Information is available free of charge at https://pubs.acs.org/doi/10.1021/acs.jpclett.0c02448.

Experimental section, computational methods, supporting results, and discussion (PDF)

■ AUTHOR INFORMATION

Corresponding Author

Masashi Unno − *Department of Chemistry and Applied Chemistry, Faculty of Science and Engineering, Saga University, Saga 840-8502, Japan;* orcid.org/0000-0002-5016-6274; Email: unno@cc.saga-u.ac.jp

Authors

Junpei Matsuo − *Department of Chemistry and Applied Chemistry, Faculty of Science and Engineering, Saga University, Saga 840-8502, Japan*

Takashi Kikukawa − *Faculty of Advanced Life Science and Global Station for Soft Matter, Global Institution for Collaborative Research and Education, Hokkaido University, Sapporo 060-0810, Japan;* orcid.org/0000-0002-6185-7281

Tomotsumi Fujisawa − *Department of Chemistry and Applied Chemistry, Faculty of Science and Engineering, Saga University, Saga 840-8502, Japan;* orcid.org/0000-0002-3282-6814

Wouter D. Hoff − *Department of Microbiology and Molecular Genetics, Oklahoma State University, Stillwater, Oklahoma 74078, United States*

Complete contact information is available at:

https://dx.doi.org/10.1021/acs.jpclett.0c02448
J. Phys. Chem. Lett. 2020, 11, 8579−8584

https://pubs.acs.org/10.1021/acs.jpclett.0c02448

Funding

This work was supported by JSPS KAKENHI grant numbers 17K07326 to T.K., 18K05037 to T.F., and 17K05756 to M.U. A portion of the computations was performed at the Research Center for Computational Science in Okazaki, Japan.

Notes

The authors declare no competing financial interest.

■ ACKNOWLEDGMENTS

We thank Takeshi Hanamoto for his help with DFT calculations on a model compound.

■ REFERENCES

(1) Rocha-Rinza, T.; Sneskov, K.; Christiansen, O.; Ryde, U.; Kongsted, J. Unraveling the Similarity of the Photoabsorption of Deprotonated *p*-Coumaric Acid in the Gas Phase and within the Photoactive Yellow Protein. *Phys. Chem. Chem. Phys.* **2011**, *13* (4), 1585−1589.

(2) Sekharan, S.; Morokuma, K. QM/MM Study of the Structure, Energy Storage, and Origin of the Bathochromic Shift in Vertebrate and Invertebrate Bathorhodopsins. *J. Am. Chem. Soc.* **2011**, *133* (13), 4734−4737.

(3) Kukura, P.; McCamant, D. W.; Yoon, S.; Wandschneider, D. B.; Mathies, R. A. Structural Observation of the Primary Isomerization in Vision with Femtosecond-Stimulated Raman. *Science* **2005**, *310* (5750), 1006−1009.

(4) Nango, E.; Royant, A.; Kubo, M.; Nakane, T.; Wickstrand, C.; Kimura, T.; Tanaka, T.; Tono, K.; Song, C.; Tanaka, R.; Arima, T.; Yamashita, A.; Kobayashi, J.; Hosaka, T.; Mizohata, E.; Nogly, P.; Sugahara, M.; Nam, D.; Nomura, T.; Shimamura, T.; Im, D.; Fujiwara, T.; Yamanaka, Y.; Jeon, B.; Nishizawa, T.; Oda, K.; Fukuda, M.; Andersson, R.; Båth, P.; Dods, R.; Davidsson, J.; Matsuoka, S.; Kawatake, S.; Murata, M.; Nureki, O.; Owada, S.; Kameshima, T.; Hatsui, T.; Joti, Y.; Schertler, G.; Yabashi, M.; Bondar, A.-N.; Standfuss, J.; Neutze, R.; Iwata, S. A Three-Dimensional Movie of Structural Changes in Bacteriorhodopsin. *Science* **2016**, *354* (6319), 1552−1557.

(5) Warshel, A.; Barboy, N. Energy Storage and Reaction Pathways in the First Step of the Vision Process. *J. Am. Chem. Soc.* **1982**, *104* (6), 1469−1476.

(6) Blanch, E. W.; Hecht, L.; Barron, L. D. Vibrational Raman Optical Activity of Proteins, Nucleic Acids, and Viruses. *Methods* **2003**, *29* (2), 196−209.

(7) He, Y.; Wang, B.; Dukor, R. K.; Nafie, L. A. Determination of Absolute Configuration of Chiral Molecules Using Vibrational Optical Activity: A Review. *Appl. Spectrosc.* **2011**, *65* (7), 699−723.

(8) Parchaňský, V.; Kapitán, J.; Bouř, P. Inspecting Chiral Molecules by Raman Optical Activity Spectroscopy. *RSC Adv.* **2014**, *4*, 57125−57136.

(9) Krupová, M.; Kessler, J.; Bouř, P. Recent Trends in Chiroptical Spectroscopy: Theory and Applications of Vibrational Circular Dichroism and Raman Optical Activity. *ChemPlusChem* **2020**, *85* (3), 561−575.

(10) Fujisawa, T.; Unno, M. Vibrational Optical Activity Spectroscopy. In *Molecular and Laser Spectroscopy Advances and Applications: Vol. 2*; Gupta, V. P., Ozaki, Y., Eds.; Elsevier, 2020; pp 41−82. DOI: 10.1016/B978-0-12-818870-5.00002-2.

(11) Nafie, L. A. *Vibrational Optical Activity: Principles and Applications*; John Wiley & Sons Ltd.: West Sussex, 2011.

(12) Unno, M.; Kikukawa, T.; Kumauchi, M.; Kamo, N. Exploring the Active Site Structure of a Photoreceptor Protein by Raman Optical Activity. *J. Phys. Chem. B* **2013**, *117* (5), 1321−1325.

(13) Shingae, T.; Kubota, K.; Kumauchi, M.; Tokunaga, F.; Unno, M. Raman Optical Activity Probing Structural Deformations of the 4-Hydroxycinnamyl Chromophore in Photoactive Yellow Protein. *J. Phys. Chem. Lett.* **2013**, *4* (8), 1322−1327.

(14) Kubota, K.; Shingae, T.; Foster, N. D.; Kumauchi, M.; Hoff, W. D.; Unno, M. Active Site Structure of Photoactive Yellow Protein with a Locked Chromophore Analogue Revealed by Near-Infrared Raman Optical Activity. *J. Phys. Chem. Lett.* **2013**, *4* (18), 3031−3038.

(15) Fujisawa, T.; Leverenz, R. L.; Nagamine, M.; Kerfeld, C. A.; Unno, M. Raman Optical Activity Reveals Carotenoid Photoactivation Events in the Orange Carotenoid Protein in Solution. *J. Am. Chem. Soc.* **2017**, *139* (30), 10456−10460.

(16) Haraguchi, S.; Shingae, T.; Fujisawa, T.; Kasai, N.; Kumauchi, M.; Hanamoto, T.; Hoff, W. D.; Unno, M. Spectroscopic Ruler for Measuring Active-Site Distortions Based on Raman Optical Activity of a Hydrogen out-of-Plane Vibration. *Proc. Natl. Acad. Sci. U. S. A.* **2018**, *115* (35), 8671−8675.

(17) Miranda, M. R. M.; Choi, A. R.; Shi, L.; Bezerra, A. G.; Jung, K.-H.; Brown, L. S. The Photocycle and Proton Translocation Pathway in a Cyanobacterial Ion-Pumping Rhodopsin. *Biophys. J.* **2009**, *96* (4), 1471−1481.

(18) Inoue, K.; Ono, H.; Abe-Yoshizumi, R.; Yoshizawa, S.; Ito, H.; Kogure, K.; Kandori, H. A Light-Driven Sodium Ion Pump in Marine Bacteria. *Nat. Commun.* **2013**, *4* (1), 1−10.

(19) Morizumi, T.; Ou, W.-L.; Eps, N. V.; Inoue, K.; Kandori, H.; Brown, L. S.; Ernst, O. P. X-Ray Crystallographic Structure and Oligomerization of *Gloeobacter* Rhodopsin. *Sci. Rep.* **2019**, *9* (1), 1−14.

(20) Kato, H. E.; Inoue, K.; Abe-Yoshizumi, R.; Kato, Y.; Ono, H.; Konno, M.; Hososhima, S.; Ishizuka, T.; Hoque, M. R.; Kunitomo, H.; Ito, J.; Yoshizawa, S.; Yamashita, K.; Takemoto, M.; Nishizawa, T.; Taniguchi, R.; Kogure, K.; Maturana, A. D.; Iino, Y.; Yawo, H.; Ishitani, R.; Kandori, H.; Nureki, O. Structural Basis for Na^+ Transport Mechanism by a Light-Driven Na^+ Pump. *Nature* **2015**, *521* (7550), 48−53.

(21) Gushchin, I.; Shevchenko, V.; Polovinkin, V.; Kovalev, K.; Alekseev, A.; Round, E.; Borshchevskiy, V.; Balandin, T.; Popov, A.; Gensch, T.; Fahlke, C.; Bamann, C.; Willbold, D.; Büldt, G.; Bamberg, E.; Gordeliy, V. Crystal Structure of a Light-Driven Sodium Pump. *Nat. Struct. Mol. Biol.* **2015**, *22* (5), 390−395.

(22) Kaledhonkar, S.; Hara, M.; Stalcup, T. P.; Xie, A.; Hoff, W. D. Strong Ionic Hydrogen Bonding Causes a Spectral Isotope Effect in Photoactive Yellow Protein. *Biophys. J.* **2013**, *105* (11), 2577−2585.

(23) Smith, S. O.; Braiman, M. S.; Myers, A. B.; Pardoen, J. A.; Courtin, J. M. L.; Winkel, C.; Lugtenburg, J.; Mathies, R. A. Vibrational Analysis of the *all-trans*-Retinal Chromophore in Light-Adapted Bacteriorhodopsin. *J. Am. Chem. Soc.* **1987**, *109* (10), 3108−3125.

(24) Kajimoto, K.; Kikukawa, T.; Nakashima, H.; Yamaryo, H.; Saito, Y.; Fujisawa, T.; Demura, M.; Unno, M. Transient Resonance Raman Spectroscopy of a Light-Driven Sodium-Ion-Pump Rhodopsin from *Indibacter Alkaliphilus*. *J. Phys. Chem. B* **2017**, *121* (17), 4431−4437.

(25) Iizuka, A.; Kajimoto, K.; Fujisawa, T.; Tsukamoto, T.; Aizawa, T.; Kamo, N.; Jung, K.-H.; Unno, M.; Demura, M.; Kikukawa, T. Functional Importance of the Oligomer Formation of the Cyanobacterial H^+ Pump *Gloeobacter* Rhodopsin. *Sci. Rep.* **2019**, *9* (1), 1−12.

(26) Haraguchi, S.; Hara, M.; Shingae, T.; Kumauchi, M.; Hoff, W. D.; Unno, M. Experimental Detection of the Intrinsic Difference in Raman Optical Activity of a Photoreceptor Protein under Preresonance and Resonance Conditions. *Angew. Chem., Int. Ed.* **2015**, *54* (39), 11555−11558.

(27) Kovalev, K.; Astashkin, R.; Gushchin, I.; Orekhov, P.; Volkov, D.; Zinovev, E.; Marin, E.; Rulev, M.; Alekseev, A.; Royant, A.; Carpentier, P.; Vaganova, S.; Zabelskii, D.; Baeken, C.; Sergeev, I.; Balandin, T.; Bourenkov, G.; Carpena, X.; Boer, R.; Maliar, N.; Borshchevskiy, V.; Büldt, G.; Bamberg, E.; Gordeliy, V. Molecular Mechanism of Light-Driven Sodium Pumping. *Nat. Commun.* **2020**, *11* (1), 2137.

(28) Smith, S. O.; Marvin, M. J.; Bogomolni, R. A.; Mathies, R. A. Structure of the Retinal Chromophore in the hR_{578} Form of Halorhodopsin. *J. Biol. Chem.* **1984**, *259* (20), 12326−12329.
(29) Nafie, L. A. Theory of Resonance Raman Optical Activity: The Single Electronic State Limit. *Chem. Phys.* **1996**, *205* (3), 309−322.

https://dx.doi.org/10.1021/acs.jpclett.0c02448
J. Phys. Chem. Lett. 2020, 11, 8579−8584